ACS OMEGA

http://pubs.acs.org/journal/acsodf

Article

Pulicaria undulata Extract-Mediated Eco-Friendly Preparation of TiO_2 Nanoparticles for Photocatalytic Degradation of Methylene Blue and Methyl Orange

Khaleel Al-hamoud, Mohammed Rafi Shaik, Merajuddin Khan,* Hamad Z. Alkhathlan, Syed Farooq Adil, Mufsir Kuniyil, Mohamed E. Assal, Abdulrahman Al-Warthan, Mohammed Rafiq H. Siddiqui, Muhammad Nawaz Tahir, Shams Tabrez Khan, Ahmad Amine Mousa, and Mujeeb Khan*

Cite This: *ACS Omega* 2022, 7, 4812−4820

Read Online

ACCESS | Metrics & More | Article Recommendations | Supporting Information

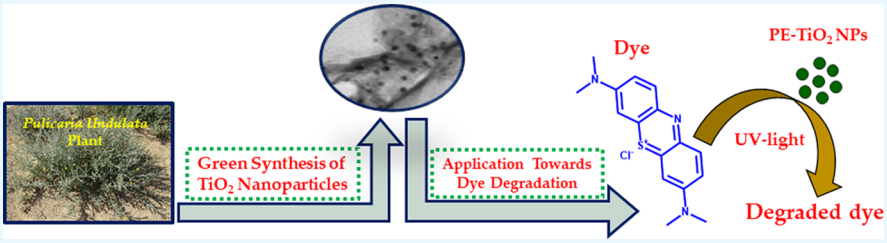

ABSTRACT: Eco-friendly approaches for the preparation of nanomaterials have recently attracted considerable attention of scientific community due to rising environmental distresses. The aim of the current study is to prepare titanium dioxide (TiO_2) nanoparticles (NPs) using an eco-friendly approach and investigate their performance for the photocatalytic degradation of hazardous organic dyes. For this, TiO_2 NPs were prepared by using the aqueous extract of the *Pulicaria undulata* (L.) plant in a single step at room temperature. Energy-dispersive X-ray spectroscopy established the presence of both titanium and oxygen in the sample. X-ray diffraction revealed the formation of crystalline, anatase-phase TiO_2 NPs. On the other hand, transmission election microscopy confirmed the formation of spherical shaped NPs. The presence of residual phytomolecules as capping/stabilization agents is confirmed by UV−vis analysis and Fourier-transform Infrared spectroscopy. Indeed, in the presence of *P. undulata*, the anatase phase of TiO_2 is stabilized at a significantly lower temperature (100 °C) without using any external stabilizing agent. The green synthesized TiO_2 NPs were used to investigate their potential for the photocatalytic degradation of hazardous organic dyes including methylene blue and methyl orange under UV−visible light irradiation. Due to the small size and high dispersion of NPs, almost complete degradation (~95%) was achieved in a short period of time (between 1 and 2 h). No significant difference in the photocatalytic activity of the TiO_2 NPs was observed even after repeated use (three times) of the photocatalyst. Overall, the green synthesized TiO_2 NPs exhibited considerable potential for fast and eco-friendly removal of harmful organic dyes.

1. INTRODUCTION

Textile mills are considered as one of the crucial sources of industrial revolution in developing nations.[1] However, they are also regarded as a great threat to the environment, which generate approximately one-fifth of world's industrial water pollution through the use of thousands of hazardous chemicals including carcinogenic compounds.[2] Moreover, textile industries also require a huge amount of water for various processes, and the liquid waste released from these sectors consists of several contaminants which cause significant environmental damage.[3] The colored wastewater released from textile industries typically contains unpleasant odor, high pH, biochemical oxygen demand, chemical oxygen demand, and a large amount of suspended solids, including a variety of inorganic salts, hazardous chemicals, and heavy metals.[4,5] Besides, the industrial effluent also contains a high concentration of toxic and carcinogenic organic dyes due to their extensive use in this sector.[6] Indeed, organic dyes have become an integral part of industrial liquid wastes due to their widespread applications in various industrial activities other than the textile sector.[7]

So far, several approaches have been applied to remove these hazardous dyes from industrial effluents including coagulation, adsorption, biodegradation, membrane process, activated

Received: September 14, 2021
Accepted: January 10, 2022
Published: February 2, 2022

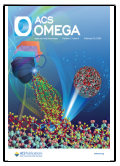

https://doi.org/10.1021/acsomega.1c05090
ACS Omega 2022, 7, 4812−4820

sludge treatment process (ASTP), and advanced oxidation process (AOP).[8,9] Each one of these processes has its own benefits and drawbacks, which are selected according to the requirement.[10] For example, mostly the effluent treatment plants apply the conventional ASTP due to its low cost; however, this method is not efficient in removing toxic organic dyes.[11,12] However, other physicochemical treatment processes, such as coagulation and adsorption, require large quantity of chemicals and hence are environmentally not suitable.[13,14]While membrane technologies including membrane bioreactors etc. are effective, these processes are less energy efficient and require high operating cost.[15] Among these processes, the AOPs have significant potential in the treatment of dye-based industrial effluent as these techniques are capable of degrading soluble organic contaminants from liquid wastes.[16−18] Particularly, heterogeneous photocatalytic degradation-based AOPs are promising methods for the degradation of organic dyes as these techniques are more effective as compared to other AOPs due to the low cost of semiconductor-based photocatalysts and high efficiency in mineralizing a variety of organic dyes.[19,20]

In this regard, nanoparticle (NP)-based semiconducting photocatalysts offer great potential for the development of AOP-based liquid waste treatment technologies. Nanomaterials including nanocrystalline transition-metal oxides offer high reactivity, great degree of flexibility for functionalization, large surface area, and other size-dependent properties.[21] To date, several semiconducting NPs have been applied as photocatalysts for the degradation of organic dyes such as, ZnO, ZrO_2, TiO_2, V_2O_5, and so forth.[22] Especially, TiO_2-based photocatalytic oxidation has been extensively applied for the degradation of organic dyes due to its stability, low cost, and optical absorption in the UV region. However, inactivity of TiO_2 in visible light due to its wide band gap (3.2 eV) seriously hindered its large-scale application which is typically addressed by band gap engineering. For example, Khan et al. have modified commercial TiO_2 NPs using electron beam treatment, which rendered them visible light activeness.[23] Apart from this, several other approaches have also been tried to enhance the photocatalytic efficiency of TiO_2 in the visible region, such as doping with transition metals, deposition of noble metal ions (Ag, Au, etc.) on the TiO_2 surface, and so forth.[24] For instance, nitrogen doping of TiO_2 fibers performed by Calisir et al. using polyvinylpyrrolidone as a carrier polymer and nitrogen source has significantly enhanced the light absorption capacity of the as-prepared sample in the visible region.[25] Apart from wide band gap, the chemical preparation of TiO_2 NPs requires specific conditions; high temperature and expensive and toxic chemicals also restrict TiO_2 applications due to serious eco-toxicological concern.

Therefore, the green synthesis of narrow-band-gap and visible-light-active TiO_2 NPs using biodegradable materials such as plant extracts, microorganisms, and enzymes is becoming increasingly popular due to its simplicity, cost-effectiveness, eco-friendly nature, and low toxicity. For example, in a recent study, Khan et al. have modified (introduced defects) commercially obtained TiO_2 NPs using a green, biogenic, and energy-efficient process in which NPs were treated in the cathode chamber of a microbial fuel cell.[26] Additionally, the preparation of semiconducting TiO_2 NPs using plant extracts has also attracted considerable attention, which minimizes the use of chemicals and other contaminants and enhances the environmental suitability of the treatment process. To date, several studies reported the application of green synthesized TiO_2 NPs for dye degradation. Still, there is continued urge for an environmental friendly preparation of TiO_2 NPs. Therefore, in the current study, TiO_2 NPs were prepared using the aqueous extract of the *Pulicaria undulata* (L.) plant using a facile, green chemistry approach. *P. undulata* is an important plant belonging to the genus *Pulicaria* and family *Asteraceae*. This plant is traditionally popular as an insect repellent, galactagogue, antiepileptic, and a tonic in folk medicine.[27] Besides, due its antibacterial and sedative activities, it has also been used for the treatment of various ailments.[28] *P. undulata* has been known to contain a variety of phytomolecules including sesquiterpenes and lactones and is also rich in certain polyphenolic contents which potentially play an important role in the biosynthesis of nanomaterials.[28,29]

Indeed, in our previous study, we have demonstrated the reducing and stabilizing potential of *P. undulata* for the synthesis of silver (Ag), gold (Au), and Au−Ag alloy NPs.[30] Herein, we have demonstrated the green synthesis of TiO_2 NPs using the *P. undulata* plant extract at a significantly lowered calcination temperature (100 °C) without using any external stabilizing agent. While in other studies, strong chemical stabilizers and high calcination temperatures (>400 °C) were required during the post treatment of NPs to obtain stable TiO_2 NPs.[31,32] However, in this case, the stabilizing ability of the phytoconstituents of *P. undulata* plant extract facilitated the formation of highly stable TiO_2 NPs at lower temperature. To confirm the successful formation of TiO_2 NPs and study their optical and morphological properties, X-ray diffraction (XRD), UV−vis, Fourier-transform infrared (FT-IR), field-emission scanning electron microscopy (SEM), energy-dispersive spectroscopy (EDS), and transmission electron microscopy (TEM) were employed. Furthermore, the photocatalytic properties of the as-prepared TiO_2 NPs were evaluated for the degradation of methyl orange (MO) and methylene blue (MB) in the presence of $NaBH_4$ at room temperature, and the progress of degradation was monitored by UV.

2. EXPERIMENTAL SECTION

2.1. Materials. Titanium(IV) isopropoxide [$Ti(OCH(CH_3)_2)_4$, 97%], MB ($C_{16}H_{18}ClN_3S$), MO ($C_{14}H_{14}N_3NaO_3S$), and sodium borohydride ($NaBH_4$) and other reagents used were purchased from Sigma-Aldrich (USA) and used without purification. Double-distilled water was used in all the experiments. Aerial parts of *P. undulata* were extracted according to the method reported in our previous study.[30] Briefly, *P. undulata* was identified by a taxonomist from King Saud University. The aerial parts of fresh *P. undulata* were cut into small pieces and dried at room temperature for 15 days in the shade. The dried and powdered aerial parts (343 g) of *P. undulata* were extracted for 3 h with boiling water. The aqueous extract was cooled and filtered through Whatman filter paper. After drying at 50 °C in vacuo in a rotary evaporator, 24.0 g of dark brown powdered water extract was obtained and used for the subsequent synthesis of TiO_2 particles. For the synthesis of TiO_2 NPs, plant extract was used from the previously prepared stock solution which was obtained by dissolving 10 mg of PE powder in 1 mL of Milli-Q water.

2.2. Preparation of TiO_2 NPs. Green synthesis of TiO_2 NPs was performed according to the following procedure, as

https://doi.org/10.1021/acsomega.1c05090
ACS Omega 2022, 7, 4812−4820

Scheme 1. Facile Green Synthesis of TiO_2 NPs Using the Aqueous Extract of *P. undulata* and Their Application as Photocatalysts toward the Degradation of Dyes

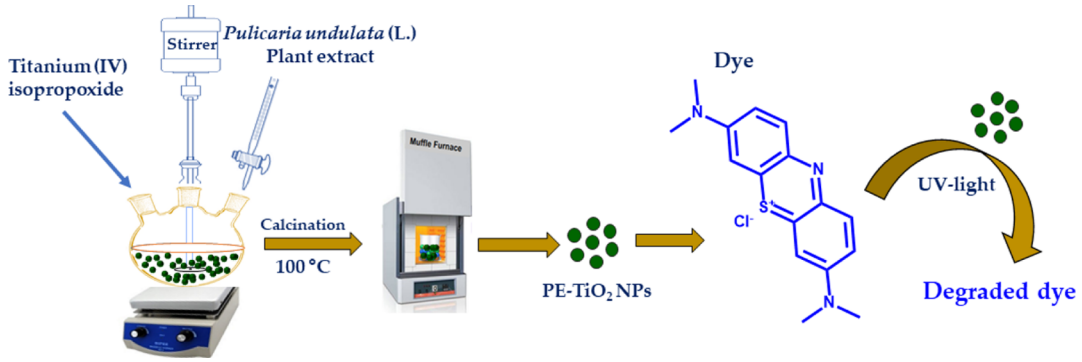

shown schematically in Scheme 1. Briefly, 200 mL of distilled water was taken in 500 mL conical flask, and its pH was adjusted to 1.5 using a required amount of diluted HCl. To this solution, a separately prepared mixture of titanium(IV) isopropoxide (5 mL) and isopropanol (50 mL) was slowly added under stirring using a dropping funnel. The resulting solution was allowed to stir for 45 min at room temperature. Subsequently, 5 mL of *P. undulata* PE from the previously prepared stock solution was added to the mixture and stirring was continued for an additional 30 min. Thereafter, stirring was stopped and the as-obtained sol was sonicated for 90 min (80 MHz). Then, water was evaporated in a hot air oven at 100 °C for 24 h and dry gel was obtained. Finally, the gel was dried at 100 °C in a furnace, which resulted in the formation of plant extract-stabilized TiO_2 NPs (PE-TiO_2). Similarly, the procedure and parameters were adopted to prepare TiO_2 NPs (TiO_2) in the absence of PE. However, in the place of PE, 1 mL of 0.05 M hydrazine hydrate was added. In this case, the sample was calcined in a furnace at different temperatures (100 and 400 °C).

2.3. Characterization of PE-TiO_2 and TiO_2 NPs. Powder XRD patterns were recorded using a Bruker diffractometer [Cu Kα (λ = 1.5406 Å) X-ray source] (D2-Phaser, Bruker, Germany). The phase of TiO_2 was confirmed by comparison of major peak positions reported in standard JCPDS database. SEM, TEM, and energy-dispersive X-ray (EDX) spectroscopy were carried out on Jeol, JED-2200 series (Akishima, Tokyo 196-8558, Japan) and Jeol TEM model JEM-1011 (Japan) at 100 keV, respectively. UV spectroscopy was performed on a Lambda 35 UV−Vis spectrophotometer (PerkinElmer, Waltham, MA, USA) in quartz cuvettes using distilled water as the reference solvent. The samples were prepared by diluting 1 mL of the NP reaction solution (collected during and at the end of the reaction) in 9 mL of water. FT-IR spectra were recorded on a PerkinElmer Spectrum 100 FT-IR spectrometer (FT-IR, PerkinElmer, Waltham, MA, USA) in the transmittance mode in the 400−4000 cm^{-1} range.

2.4. Photocatalytic Degradation of Dyes. The photocatalytic degradation of MB and MO was performed by the addition 1 mL of 0.01 M $NaBH_4$ solution into 30 mL of 10^{-3} M MB and MO solutions under stirring, respectively. After sometime (5 min), 100 mg of PE-TiO_2 was added, and the as-prepared mixture was irradiated with a 24 W Philips light-emitting diode (LED) lamp (λ > 400 nm) which was kept at a distance of ∼10 cm from the mixture. The solution was stirred continuously until the reaction was complete (change in the color of the reaction solution indicates the completion of the reaction). For the kinetic study of the degradation of MB and MO, a small amount of the sample was taken out at regular intervals and analyzed using UV−vis spectroscopy. Reusability of PE-TiO_2 was tested by performing repeated (three times) photocatalytic degradation of MB under similar aforementioned conditions. All the reactions were performed for 1 h, and after every reaction, the catalyst was separated via centrifugation, washed with deionized water, and reused.

3. RESULTS AND DISCUSSION

Two different samples of TiO_2 NPs were prepared in the presence (PE-TiO_2) and absence (TiO_2) of *P. undulata* PE to study the effect of plant extract on the preparation of NPs. In the presence of plant extract, TiO_2 NPs were formed at a much lower calcination temperature (100 °C) without using any external reducing and/or stabilizing agent. Whereas under similar conditions in the absence of plant extract, the formation of TiO_2 NPs did not occur. However, TiO_2 NPs were also formed in the absence of PE, when $NaBH_4$ was used during the preparation in the place of PE and when the sample was calcined at a high temperature of 400 °C.

Initially, the preparation of TiO_2 NPs under different conditions was confirmed by XRD analysis. The XRD patterns of TiO_2 NPs with PE (PE-TiO_2), without PE (TiO_2-100 °C), and NPs obtained by using $NaBH_4$ and at a high calcination temperature (TiO_2-400 °C) are shown in Figure 1. The results reveal the successful formation of crystalline, anatase phase of TiO_2 NPs in the case of PE-TiO_2 (green line, Figure 1) and

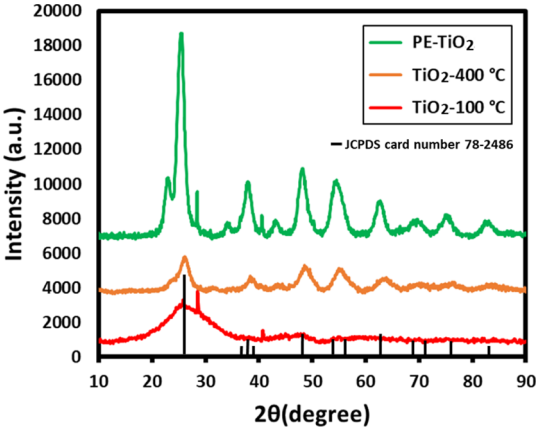

Figure 1. XRD patterns of TiO_2 NPs prepared by using different reaction conditions and calcination temperatures.

https://doi.org/10.1021/acsomega.1c05090
ACS Omega 2022, 7, 4812−4820

TiO_2-400 °C (orange line, Figure 1). However, the XRD pattern of TiO_2-100 °C (red line, Figure 1) which was prepared without using PE did not exhibit characteristic reflection (consists of few broad reflections) due to the absence of TiO_2 NPs in the sample. Notably, the XRD reflections in PE-TiO_2 (green line, Figure 1) are much sharper when compared to the reflection of TiO_2-400 °C (orange line, Figure 1), pointing toward the formation of a highly crystalline sample in the presence of PE. This could be due to the effective stabilization of NPs by the phytomolecules of plant extract. The average crystallite size of the PE-TiO_2 NPs was calculated by Debye Scherrer's equation.

$$\text{Debye} - \text{Scherer's equation } d = \frac{k\lambda}{\beta \cos\theta} \quad (1)$$

where d is the NP's average mean diameter, λ is the wavelength, and β is the angular full width at half-maximum of the peaks. The average crystallite size of the PE-TiO_2 NPs was found to be ∼7 nm. The XRD pattern of PE-TiO_2 NPs exhibited several reflections at different 2θ angles such as 25.51, 38.05, 48.41, 54.83, 62.95, 70.64, and 75.55° which correspond to the miller indices (hkl) of (1 0 1), (0 0 4), (2 0 0), (2 1 1), (2 0 4), (2 2 0), and (2 1 5), respectively. This clearly matched with the anatase phase of TiO_2 NPs reported in the XRD database (JCPDS card no. 78-2486).[33] These results confirm that *P. undulata* PE facilitated the formation of the anatase phase of highly crystalline TiO_2 NPs at a much lower calcination temperature (calcined at 100 °C for 3 h) when compared to the chemically synthesized NPs (TiO_2-400 °C). Indeed, the sharp reflections in the XRD of PE-TiO_2 point toward the high crystallinity of the green synthesized TiO_2 NPs, which possibly enhances the photocatalytic activity of the sample.[34]

The stabilization of green synthesized TiO_2 NPs by the phytomolecules of PE is confirmed by both UV−vis and FT-IR spectroscopies. For the purpose of comparison, UV spectra of pure *P. undulata* PE (green line, Figure 2), PE-TiO_2 (red line, Figure 2), and TiO_2-400 °C (blue line, Figure 2) were measured, as shown in Figure 2. The UV spectrum of pure PE consists of two characteristic peaks at 285 and 328 nm due to the presence of phenolics and other phytomolecules.[28,35] However, pristine TiO_2 NPs typically exhibit a characteristic absorption peak in the range of 320−350 nm.[36] The UV spectrum of PE-TiO_2 consists of two different absorption peaks at 288 and 329 nm, which are similar to the peaks of pure PE, indicating the presence of phytomolecules of *P. undulata* PE as stabilizing ligands on the surface of TiO_2 NPs. Notably, the characteristic UV peak of TiO_2 NPs is not clearly visible in the UV spectrum of PE-TiO_2 due to the overlapping of peaks in the similar region between 320 and 350 nm. While the peak at 330 nm in the UV spectrum of TiO_2-400 °C confirms the formation of TiO_2 NPs by the chemical method, the absence of UV peaks belonging to the PE further assures the successful stabilization of TiO_2 NPs by PE phytomolecules in PE-TiO_2.

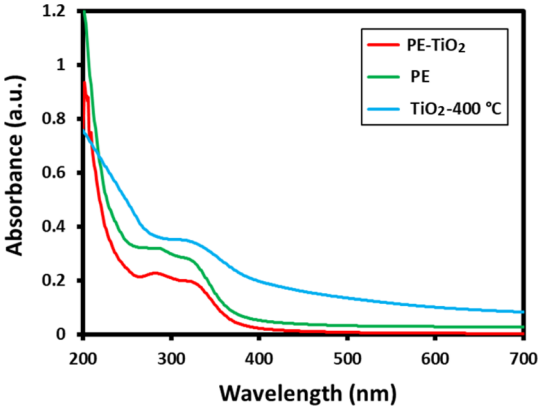

Figure 2. UV−vis spectra of *P. undulata* PE (green line), PE-TiO_2 (red line), and TiO_2-400 °C (blue line).

Additionally, FT-IR analysis of PE, PE-TiO_2, and TiO_2-400 °C were also performed to recognize the possible phytomolecules based on the identification of chemical groups present in the *P. undulata* PE, as shown in Figure 3. The PE showed a broad absorption between 3800 and 3300 cm^{-1} and sharp bands at ∼2929 and 2850 cm^{-1}, corresponding to the O−H and C−H stretches (red line, Figure 3), respectively. Peaks at 1753, 1620, and 1405 cm^{-1} can be attributed to C−H deformations and C−C and C−O stretches, respectively. However, 1264 and 1059 cm^{-1} peaks represent C−O stretches of alcohol and ether groups, respectively. Possibly, these functional groups indicate the presence of phenolic and flavonoid groups in the *P. undulata* PE, which may be responsible for the reduction and/or capping of metallic ions (Ti^{4+}) of the starting material, and play a crucial role during the eco-friendly preparation of TiO_2 NPs. Indeed, majority of the IR peaks present in the PE also exist in the IR spectrum of PE-TiO_2 (green line, Figure 3) with slight shifts and reduced intensities. This confirms the dual role of *P. undulata* PE for the reduction and surface stabilization of resulting NPs. On the other hand, no such peaks are found in the IR spectrum of chemically synthesized TiO_2 NPs (TiO_2-400 °C). The IR spectrum of TiO_2-400 °C (blue line, Figure 3) exhibits a wide peak at ∼3425 cm^{-1} together with a small and sharp peak at ∼1630 cm^{-1}, which possibly represents the existence of the OH group and surface-adsorbed water molecules, respectively.[37] Besides, a broad peak in the range of 500−700 cm^{-1} can be attributed to Ti−O stretching and Ti−O−Ti bridging stretching modes.[38] These peaks may also indicate the formation of an anatase phase of TiO_2 NPs, which is reported to exhibit an IR peak at 652 cm^{-1}.[39] Markedly, the absence of

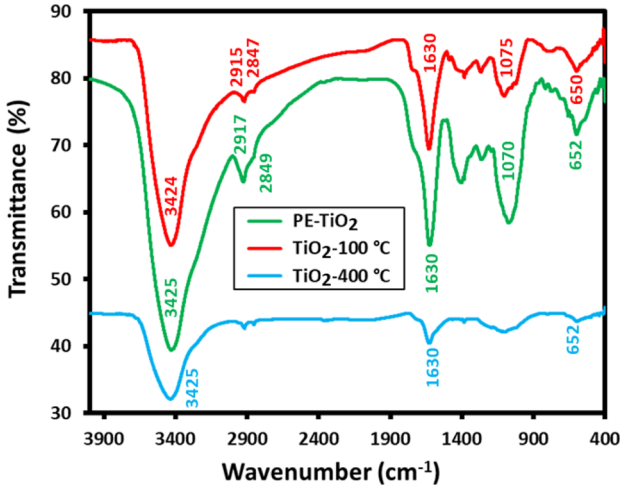

Figure 3. FT-IR spectra of plant extract (green line), PE-TiO_2 (red line), and TiO_2-400 °C prepared at higher calcination temperature without using PE (blue line).

https://doi.org/10.1021/acsomega.1c05090
ACS Omega 2022, 7, 4812−4820

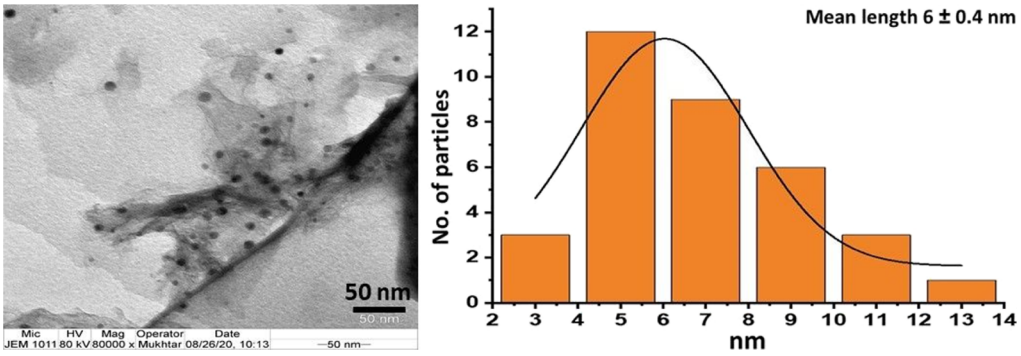

Figure 4. TEM analysis and particle size distribution of PE-TiO_2 NPs.

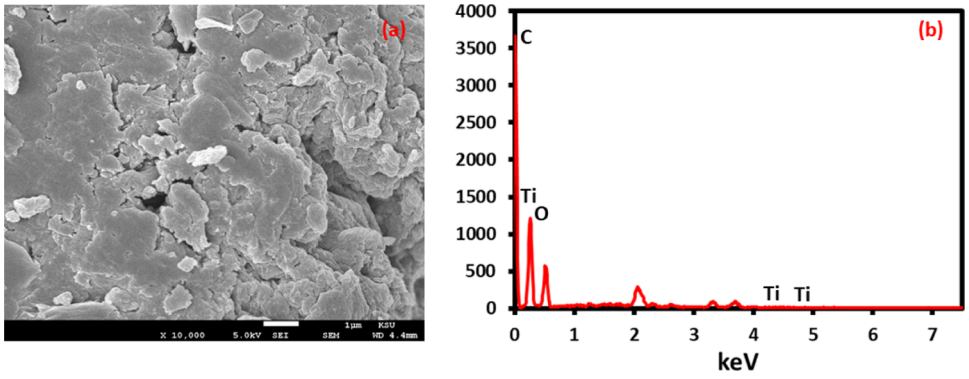

Figure 5. (a) SEM analysis and (b) EDX analysis of PE-TiO_2 NPs.

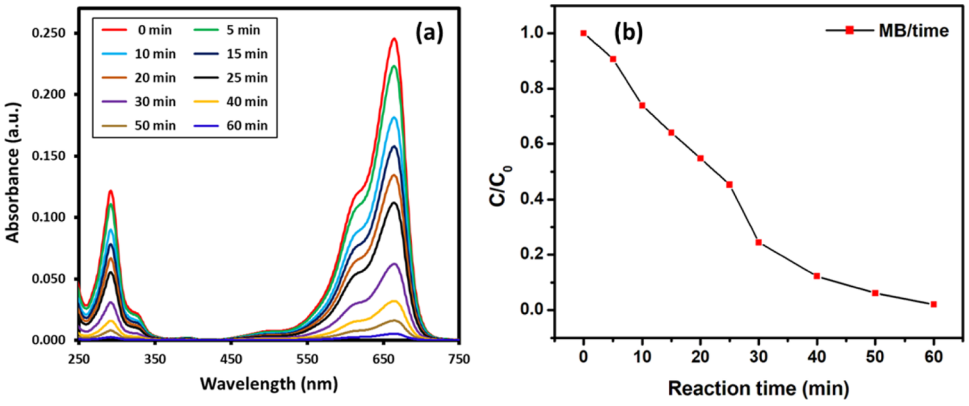

Figure 6. (a) Photocatalytic activity of green synthesized PE-TiO_2 NPs was evaluated toward the degradation of MB, and (b) kinetic profiles of the photocatalytic degradation of MB under lamp irradiation [24 W Philips LED lamp (λ > 400 nm)] using PE-TiO_2 NPs.

characteristic peaks between 2900 and 3000 cm^{-1} belonging to C−H stretching points toward the removal of organic compounds from TiO_2-400 °C due to high calcination temperature.

After confirming the synthesis and stabilization of green synthesized TiO_2, PE-TiO_2 was subjected to microscopic characterization including TEM, SEM, and EDX. The morphology of the PE-TiO_2 NPs was analyzed by TEM. Figure 4 shows spherical-shaped, slightly irregularly sized nanocrystalline TiO_2 NPs in the size range of 5−20 nm, which also confirm grain sizes estimated by XRD. The SEM images were also recorded to determine the morphology and average grain size of the NPs. The SEM images shown in Figure 5a also indicate the spherical-shaped TiO_2 NPs with a diameter ranging from ∼5 to 25 nm. Clearly, a considerable number of small and distinct TiO_2 NPs can be seen along with some relatively larger-sized well-dispersed NPs. The high-quality dispersion of PE-TiO_2 can be attributed to the residual phytoconstituents of *P. undulata* PE, such as flavonoids, polyphenols, alkaloids, and so forth, which have facilitated the stabilization of the resulting TiO_2 NPs and thus enhanced the dispersion of NPs by inhibiting their agglomeration. In addition, EDS was used to determine the elemental composition of PE-TiO_2 NPs. The EDX spectrum in Figure 5b revealed the composition of the sample, which includes both Ti (titanium) and O (oxygen). Besides, the presence of carbon contents at 222 eV and a large percentage of oxygen can be attributed to the phytomolecules of PE remained on the surface of TiO_2 NPs as stabilizing ligands.

3.1. Photocatalytic Degradation of MB and MO. The photocatalytic activity of green synthesized PE-TiO_2 NPs was evaluated toward the degradation of two different organic dyes

https://doi.org/10.1021/acsomega.1c05090
ACS Omega 2022, 7, 4812−4820

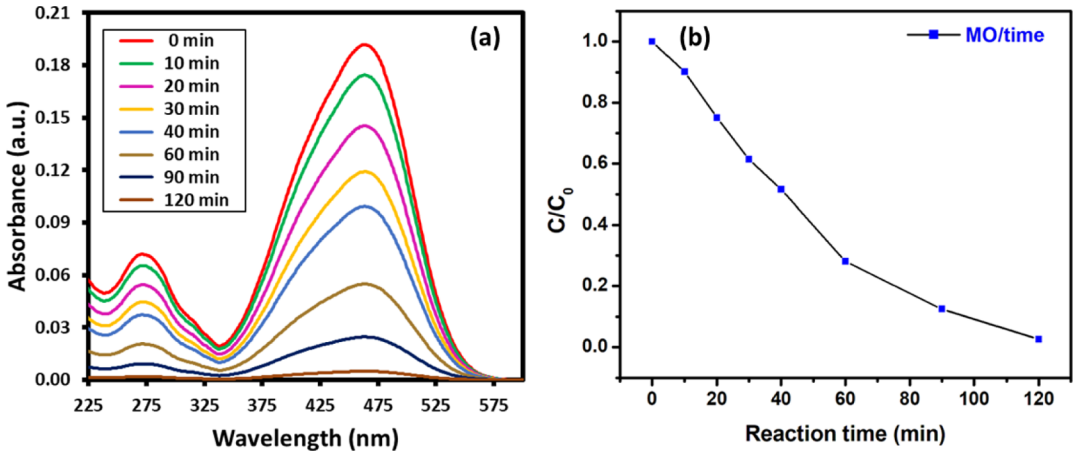

Figure 7. (a) Catalytic activity of green synthesized PE-TiO_2 NPs was evaluated toward the degradation of MO, and (b) Kinetic profiles of the photocatalytic degradation of MO under lamp irradiation [24 W Philips LED lamp (λ > 400 nm)] using PE-TiO_2 NPs.

Table 1. Comparison of the PE-TiO_2 Photocatalyst for the Dye Degradation Comparable with the Other TiO_2-Based Photocatalysts Reported in the Literature

s. no	type of photocatalyst	method of preparation	type of dye	time of reaction (min)	degradation (%)	literature
1	flower-shaped TiO_2	hydrothermal	MB	180	~90	42
2	TiO_2/activated carbon	chemical method	MB	90	~92	43
3	TiO_2/Ag	chemical method	MB	30	~95	31
4	TiO_2	green synthesized	MB	60	~95	in this study
5	TiO_2	sol−gel method	MO	130	~90	44
6	TiO_2	sol−gel method	MO	60	~60	45
7	TiO_2	hydrothermal method	MO	120	~55	46
8	TiO_2	green synthesized	MO	120	~95	in this study

including MB shown in Figure 6a,b and MO shown in Figure 7a,b using 1 mL of 0.01 M $NaBH_4$ solution. These dyes were selected as they show different colors before and after degradation, which is helpful to confirm the completion of the reaction. MB belongs to a category of cationic thiazine dye which is applied in several fields including chemical and biomedical applications. MB demonstrates deep blue color in its oxidized state in the aqueous solution and is colorless when reduced (leuco form).[40] The UV spectrum of MB exhibits absorption peaks at 290 and 664 nm due to $\pi \rightarrow \pi^*$ and $n \rightarrow \pi^*$ transitions, which can be used to monitor the reduction of dye. On the other hand, MO is an azo dye and typically used as an indicator in several applications. MO is orange red in color in the aqueous solution and exhibits strong absorption peaks at 464 nm due to the presence of the −N═N− group.[41]

In case of the degradation of both MB and MO, $NaBH_4$ is used, which is a strong reducing agent; however, it is not sufficient to complete the reactions due to the difference in redox potential, which makes them kinetically forbidden. To prove this point, the degradation reactions were performed using $NaBH_4$ as reducing agents in both the presence and absence of the PE-TiO_2 nanocatalyst. In the absence of nanocatalysts (blank experiment), both the color and the intensity of the characteristic absorption peaks of MB (664 nm) and MO (464 nm) were slightly changed after a long time (several hours). This indicates that $NaBH_4$ is not capable of degrading dyes individually. However, in the presence of the PE-TiO_2 photocatalyst, the rate of degradation significantly increased, even with the addition of a small amount of the catalyst. Indeed, the photocatalytic activity of PE-TiO_2 is either slightly better or comparable to the other TiO_2-based photocatalysts reported in the literature (cf. Table 1). Upon the addition of photocatalysts in both cases, the color of the reactions gradually changed to colorless in a short period of time. This is also reflected in their UV spectra, where the intensity of the characteristic λ_{max} gradually decreased upon increasing the reaction time. To make the degradation reactions eco-friendlier, we tried to replace $NaBH_4$ with *P. undulata* PE due to its good reducing potential. For this purpose, several experiments were conducted using *P. undulata* PE instead of $NaBH_4$, in both the presence and absence of the PE-TiO_2 nanocatalyst (data not shown here). However, in this case, the degradation of dyes did not occur even after using the PE-TiO_2 photocatalyst. This shows that the reducing potential of *P. undulata* PE is not sufficient to proceed the dye degradation reaction. Prior to all photocatalytic degradation reactions, the reaction mixture containing dye and catalysts was stirred under darkness for 30 min to achieve adsorption equilibrium.

The time-dependent degradation of MB under irradiation is demonstrated in Figure 6. In this case, within an hour of irradiation, in the presence of the PE-TiO_2 nanocatalyst, the intensity of the characteristic absorption peak of MB at 664 nm gradually decreased and almost disappeared after 60 min. This indicated the degradation of MB (~95%), which is also reflected by the change in the color of the solution from blue to colorless. In addition, the kinetic profiles for the photocatalytic degradation of both dyes are calculated with respect to time and shown in Figures 6b and 7b. Both figures show the relative rate of degradation versus time. MB almost degraded after 60 min, whereas the same concentration of MO took almost 120 min. The concentration of each pollutant

https://doi.org/10.1021/acsomega.1c05090
ACS Omega 2022, 7, 4812−4820

(organic dye) could be monitored at a given time. Similarly, the degradation of MO was also performed in the presence of the PE-TiO_2 nanocatalyst. The UV spectrum of MO exhibits two characteristic absorption bands at 464 and 272 nm, which are attributed to the azo bond and phenyl ring of the MO. Upon irradiation, these bands decrease due to the dissociation of azo bonds and the phenyl ring, which leads to the degradation and mineralization of MO.[47] Also, in this case, without the PE-TiO_2 photocatalyst, the degradation process was very slow, whereas in the presence of the catalyst, complete decolorization of the dye was achieved in a short period of time. As shown in Figure 7, due to photoirradiation, complete degradation of MO was achieved in 120 min (~95%) in the presence of the PE-TiO_2 nanocatalyst, whereas without the nanocatalyst, the degradation was almost negligible. In order to test the reusability of the PE-TiO_2 photocatalyst, repeated (three cycles) photocatalytic degradation of MB was performed under similar reaction conditions. After every reaction, the catalyst was separated via centrifugation, washed with water, and reused. Even after repeated use, the activity of the photocatalyst was slightly effected, which is reflected by the marginal decrease in the degradation percentage of MB, which was recorded to be 79% in 1 h even after three cycles, as shown in Figure 8. To check the stability, after the third cycle, the

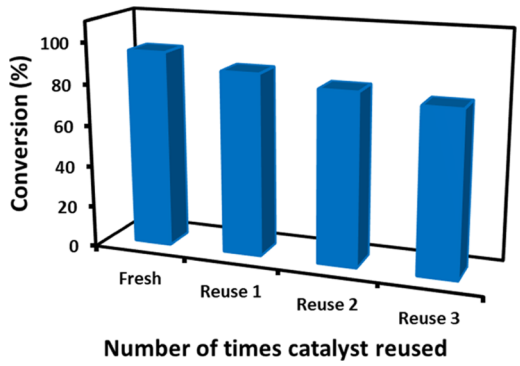

Figure 8. Reusability study of the PE-TiO_2 photocatalyst toward the degradation of MB under similar reaction conditions (room temperature, 1 h reaction time).

reused photocatalyst was characterized by SEM and XRD (cf. Figure S1, Supporting Information), which did not exhibit any major changes in the texture and phase of the photocatalyst.

4. CONCLUSIONS

Herein, we studied the synthesis of TiO_2 NPs (PE-TiO_2) using the aqueous extract of the *P. undulata* plant and their performance toward the degradation of hazardous organic dyes including MO and MB. The NPs were prepared in a single step at room temperature without using any external stabilizing ligands. In this case, the PE facilitated the formation of TiO_2 NPs at a much lowered calcination temperature (100 °C), unlike chemically synthesized TiO_2 NPs (TiO_2-400 °C). It is noteworthy that the chemical preparation of TiO_2 NPs was performed by using $NaBH_4$ as the reducing agent. In this method, a high calcination temperature of 400 °C is required during the post treatment process to obtain a stable phase of TiO_2 NPs. However, the functionalizing ability of the phytomolecules of the *P. undulata* PE helped to stabilize PE-TiO_2 NPs at a much lower calcination temperature (100 °C). The formation and morphology of PE-TiO_2 NPs are established by XRD, EDX, SEM, and TEM. However, successful stabilization of NPs by the residual phytomolecules of the PE is indicated by UV−vis and FT-IR analysis. The as-prepared PE-TiO_2 acted as an effective photocatalyst for the degradation of MB and MO under visible light irradiation. The broad-spectrum solar photocatalytic activity of the nanocatalyst can be attributed to the smaller-sized, crystalline nature of anatase-phase PE-TiO_2 NPs. Moreover, the presence of a large amount of residual phytomolecules on the surface of NPs rendered highly dispersed and stabilized TiO_2 NPs which allowed better utilization of a broad spectrum of solar radiation during photocatalysis. Therefore, the eco-friendly synthesis of TiO_2 NPs using the aqueous extract of biodegradable and nontoxic *P. undulata* PE is a promising approach to prepare other functional metal oxides. NPs can be effectively utilized to combat various environmental threats including hazardous organic dyes.

■ ASSOCIATED CONTENT

Supporting Information

The Supporting Information is available free of charge at https://pubs.acs.org/doi/10.1021/acsomega.1c05090.

Figure S1: (a) SEM analysis and (b) XRD analysis of reused photocatalyst PE-TiO2 NPs (PDF)

■ AUTHOR INFORMATION

Corresponding Authors

Merajuddin Khan − *Department of Chemistry, College of Science, King Saud University, Riyadh 11451, Saudi Arabia;* orcid.org/0000-0002-0087-0669; Email: mkhan3@ksu.edu.sa

Mujeeb Khan − *Department of Chemistry, College of Science, King Saud University, Riyadh 11451, Saudi Arabia;* orcid.org/0000-0002-4088-6913; Email: kmujeeb@ksu.edu.sa

Authors

Khaleel Al-hamoud − *Department of Chemistry, College of Science, King Saud University, Riyadh 11451, Saudi Arabia*

Mohammed Rafi Shaik − *Department of Chemistry, College of Science, King Saud University, Riyadh 11451, Saudi Arabia;* orcid.org/0000-0003-2937-317X

Hamad Z. Alkhathlan − *Department of Chemistry, College of Science, King Saud University, Riyadh 11451, Saudi Arabia*

Syed Farooq Adil − *Department of Chemistry, College of Science, King Saud University, Riyadh 11451, Saudi Arabia;* orcid.org/0000-0002-2768-1235

Mufsir Kuniyil − *Department of Chemistry, College of Science, King Saud University, Riyadh 11451, Saudi Arabia;* orcid.org/0000-0001-8038-1381

Mohamed E. Assal − *Department of Chemistry, College of Science, King Saud University, Riyadh 11451, Saudi Arabia*

Abdulrahman Al-Warthan − *Department of Chemistry, College of Science, King Saud University, Riyadh 11451, Saudi Arabia*

Mohammed Rafiq H. Siddiqui − *Department of Chemistry, College of Science, King Saud University, Riyadh 11451, Saudi Arabia;* orcid.org/0000-0002-4703-0333

Muhammad Nawaz Tahir − *Department of Chemistry, King Fahd University of Petroleum & Minerals, Dhahran 31261, Saudi Arabia; Interdisciplinary Research Center for-Hydrogen and Energy Storage (IRC-HES), King Fahd*

https://doi.org/10.1021/acsomega.1c05090
ACS Omega 2022, 7, 4812−4820

University of Petroleum and & Minerals, Dhahran 31261, Saudi Arabia

Shams Tabrez Khan − *Department of Agricultural Microbiology, Faculty of Agricultural Sciences, Aligarh Muslim University, Aligarh 202002 Uttar Pradesh, India*

Ahmad Amine Mousa − *Department of Chemistry, College of Science, King Saud University, Riyadh 11451, Saudi Arabia*

Complete contact information is available at: https://pubs.acs.org/10.1021/acsomega.1c05090

Notes

The authors declare no competing financial interest.

■ ACKNOWLEDGMENTS

The authors extend their appreciation to the Deputyship for Research & Innovation, Ministry of Education in Saudi Arabia for funding this research work through the project number (DRI-KSU-1306).

■ REFERENCES

(1) Yan, S.; Jones, C.; Henninger, C. E.; McCormick, H. Textile industry insights towards impact of regenerated cellulosic and synthetic fibres on microfibre pollution. *Sustainability in the Textile and Apparel Industries*; Springer: Cham, 2020; pp 157−171.

(2) Jaganathan, V.; Cherurveettil, P.; Chellasamy, A.; Premapriya, M. Environmental pollution risk analysis and management in textile industry: a preventive mechanism. *Eur. Sci. J.* **2014**, *2*, 480−486.

(3) Chen, L.; Caro, F.; Corbett, C. J.; Ding, X. Estimating the environmental and economic impacts of widespread adoption of potential technology solutions to reduce water use and pollution: Application to China's textile industry. *Environ. Impact Assess. Rev.* **2019**, *79*, 106293.

(4) Khan, S.; Malik, A. Environmental and health effects of textile industry wastewater. *Environmental Deterioration and Human Health*; Springer, 2014; pp 55−71.

(5) Tounsadi, H.; Metarfi, Y.; Taleb, M.; El Rhazi, K.; Rais, Z. Impact of chemical substances used in textile industry on the employee's health: Epidemiological study. *Ecotoxicol. Environ. Saf.* **2020**, *197*, 110594.

(6) Bener, S.; Atalay, S.; Ersöz, G. The hybrid process with eco-friendly materials for the treatment of the real textile industry wastewater. *Ecol. Eng.* **2020**, *148*, 105789.

(7) Paraschiv, D.; Tudor, C.; Petrariu, R. The Textile Industry and Sustainable Development: A Holt-Winters Forecasting Investigation for the Eastern European Area. *Sustainability* **2015**, *7*, 1280−1291.

(8) Hasanbeigi, A.; Price, L. A technical review of emerging technologies for energy and water efficiency and pollution reduction in the textile industry. *J. Clean. Prod.* **2015**, *95*, 30−44.

(9) Saratale, R. G.; Banu, J. R.; Shin, H.-S.; Bharagava, R. N.; Saratale, G. D. Textile industry wastewaters as major sources of environmental contamination: bioremediation approaches for its degradation and detoxification. *Bioremediation of Industrial Waste for Environmental Safety*; Springer, 2020; pp 135−167.

(10) Nimkar, U. Sustainable chemistry: a solution to the textile industry in a developing world. *Curr. Opin. Green Sustain.* **2018**, *9*, 13−17.

(11) Meerbergen, K.; Crauwels, S.; Willems, K. A.; Dewil, R.; Van Impe, J.; Appels, L.; Lievens, B. Decolorization of reactive azo dyes using a sequential chemical and activated sludge treatment. *J. Biosci. Bioeng.* **2017**, *124*, 668−673.

(12) Villar-Navarro, E.; Baena-Nogueras, R. M.; Paniw, M.; Perales, J. A.; Lara-Martín, P. A. Removal of pharmaceuticals in urban wastewater: High rate algae pond (HRAP) based technologies as an alternative to activated sludge based processes. *Water Res.* **2018**, *139*, 19−29.

(13) Dotto, J.; Fagundes-Klen, M. R.; Veit, M. T.; Palácio, S. M.; Bergamasco, R. Performance of different coagulants in the coagulation/flocculation process of textile wastewater. *J. Clean. Prod.* **2019**, *208*, 656−665.

(14) Babaei, A. A.; Kakavandi, B.; Rafiee, M.; Kalantarhormizi, F.; Purkaram, I.; Ahmadi, E.; Esmaeili, S. Comparative treatment of textile wastewater by adsorption, Fenton, UV-Fenton and US-Fenton using magnetic nanoparticles-functionalized carbon (MNPs@C). *J. Ind. Eng. Chem.* **2017**, *56*, 163−174.

(15) Leaper, S.; Abdel-Karim, A.; Gad-Allah, T. A.; Gorgojo, P. Air-gap membrane distillation as a one-step process for textile wastewater treatment. *Chem. Eng. J.* **2019**, *360*, 1330−1340.

(16) Jing, H.-P.; Wang, C.-C.; Zhang, Y.-W.; Wang, P.; Li, R. Photocatalytic degradation of methylene blue in ZIF-8. *RSC Adv.* **2014**, *4*, 54454−54462.

(17) Wang, F.-X.; Yi, X.-H.; Wang, C.-C.; Deng, J.-G. Photocatalytic Cr(VI) reduction and organic-pollutant degradation in a stable 2D coordination polymer. *Chin. J. Catal.* **2017**, *38*, 2141−2149.

(18) Wang, F.-X.; Chen, X.; Wang, P.; Wang, C.-C. New Zn/Cd coordination polymers constructed from mixed ligands: crystal structures and photocatalytic performances toward organic dyes degradation. *J. Inorg. Organomet. Polym. Mater.* **2018**, *28*, 1565−1573.

(19) Gupta, V. K.; Saravanan, R.; Agarwal, S.; Gracia, F.; Khan, M. M.; Qin, J.; Mangalaraja, R. V. Degradation of azo dyes under different wavelengths of UV light with chitosan-SnO2 nano-composites. *J. Mol. Liq.* **2017**, *232*, 423−430.

(20) Rauf, M.; Ashraf, S. S. Fundamental principles and application of heterogeneous photocatalytic degradation of dyes in solution. *Chem. Eng. J.* **2009**, *151*, 10−18.

(21) Khan, M. E.; Khan, M. M.; Cho, M. H. Ce^{3+}-ion, surface oxygen vacancy, and visible light-induced photocatalytic dye degradation and photocapacitive performance of CeO 2-graphene nanostructures. *Sci. Rep.* **2017**, *7*, 5928.

(22) Ahmad, M.; Rehman, W.; Khan, M. M.; Qureshi, M. T.; Gul, A.; Haq, S.; Ullah, R.; Rab, A.; Menaa, F. Phytogenic fabrication of ZnO and gold decorated ZnO nanoparticles for photocatalytic degradation of Rhodamine B. *J. Environ. Chem. Eng.* **2021**, *9*, 104725.

(23) Khan, M. M.; Ansari, S. A.; Pradhan, D.; Ansari, M. O.; Han, D. H.; Lee, J.; Cho, M. H. Band gap engineered TiO_2 nanoparticles for visible light induced photoelectrochemical and photocatalytic studies. *J. Mater. Chem. A* **2014**, *2*, 637−644.

(24) Ansari, S. A.; Khan, M. M.; Ansari, M. O.; Cho, M. H. Nitrogen-doped titanium dioxide (N-doped TiO_2) for visible light photocatalysis. *New J. Chem.* **2016**, *40*, 3000−3009.

(25) Calisir, M. D.; Gungor, M.; Demir, A.; Kilic, A.; Khan, M. M. Nitrogen-doped TiO_2 fibers for visible-light-induced photocatalytic activities. *Ceram. Int.* **2020**, *46*, 16743−16753.

(26) Khan, M. E.; Khan, M. M.; Min, B.-K.; Cho, M. H. Microbial fuel cell assisted band gap narrowed TiO_2 for visible light-induced photocatalytic activities and power generation. *Sci. Rep.* **2018**, *8*, 1723.

(27) Ali, N. A. A.; Sharopov, F. S.; Alhaj, M.; Hill, G. M.; Porzel, A.; Arnold, N.; Setzer, W. N.; Schmidt, J.; Wessjohann, L. Chemical composition and biological activity of essential oil from Pulicaria undulata from Yemen. *Nat. Prod. Commun.* **2012**, *7*, 1934578X1200700238.

(28) Hussein, S. R.; Marzouk, M. M.; Soltan, M. M.; Ahmed, E. K.; Said, M. M.; Hamed, A. R. Phenolic constituents of Pulicaria undulata (L.) C.A. Mey. sub sp. undulata (Asteraceae): Antioxidant protective effects and chemosystematic significances. *J. Food Drug Anal.* **2017**, *25*, 333−339.

(29) Hegazy, M.-E. F.; Nakamura, S.; Tawfik, W. A.; Abdel-Azim, N. S.; Abdel-Lateff, A.; Matsuda, H.; Paré, P. W. Rare hydroperoxyl guaianolide sesquiterpenes from Pulicaria undulata. *Phytochem. Lett.* **2015**, *12*, 177−181.

(30) Khan, M.; Al-Hamoud, K.; Liaqat, Z.; Shaik, M. R.; Adil, S. F.; Kuniyil, M.; Alkhathlan, H. Z.; Al-Warthan, A.; Siddiqui, M. R. H.; Mondeshki, M.; Tremel, W.; Khan, M.; Tahir, M. N. Synthesis of Au, Ag, and Au−Ag Bimetallic Nanoparticles Using Pulicaria undulata

Extract and Their Catalytic Activity for the Reduction of 4-Nitrophenol. *Nanomaterials* **2020**, *10*, 1885.
(31) Naraginti, S.; Stephen, F. B.; Radhakrishnan, A.; Sivakumar, A. Zirconium and silver co-doped TiO_2 nanoparticles as visible light catalyst for reduction of 4-nitrophenol, degradation of methyl orange and methylene blue. *Spectrochim. Acta, Part A* **2015**, *135*, 814−819.
(32) Goutam, S. P.; Saxena, G.; Singh, V.; Yadav, A. K.; Bharagava, R. N.; Thapa, K. B. Green synthesis of TiO_2 nanoparticles using leaf extract of Jatropha curcas L. for photocatalytic degradation of tannery wastewater. *Chem. Eng. J.* **2018**, *336*, 386−396.
(33) Chen, J.; Zhang, L. NH_4Cl-assisted low temperature synthesis of anatase TiO_2 nanostructures from Ti powder. *Mater. Lett.* **2009**, *63*, 1797−1799.
(34) Chernyak, S. A.; Suslova, E. V.; Egorov, A. V.; Maslakov, K. I.; Savilov, S. V.; Lunin, V. V. Effect of Co crystallinity on Co/CNT catalytic activity in CO/CO_2 hydrogenation and CO disproportionation. *Appl. Surf. Sci.* **2016**, *372*, 100−107.
(35) Robbins, R. J. Phenolic acids in foods: an overview of analytical methodology. *J. Agric. Food Chem.* **2003**, *51*, 2866−2887.
(36) Pazokifard, S.; Mirabedini, S. M.; Esfandeh, M.; Mohseni, M.; Ranjbar, Z. Silane grafting of TiO_2 nanoparticles: dispersibility and photoactivity in aqueous solutions. *Surf. Interface Anal.* **2012**, *44*, 41−47.
(37) Ghali, E.; Sastri, V. S.; Elboujdaini, M. *Corrosion Prevention and Protection: Practical Solutions*; John Wiley & Sons, 2007.
(38) Peiró, A. M.; Peral, J.; Domingo, C.; Domènech, X.; Ayllón, J. A. Low-temperature deposition of TiO_2 thin films with photocatalytic activity from colloidal anatase aqueous solutions. *Chem. Mater.* **2001**, *13*, 2567−2573.
(39) Karakitsou, K. E.; Verykios, X. E. Effects of altervalent cation doping of titania on its performance as a photocatalyst for water cleavage. *J. Phys. Chem.* **1993**, *97*, 1184−1189.
(40) Small, J. M.; Hintelmann, H. Methylene blue derivatization then LC-MS analysis for measurement of trace levels of sulfide in aquatic samples. *Anal. Bioanal. Chem.* **2007**, *387*, 2881−2886.
(41) Joseph, S.; Mathew, B. Microwave-assisted green synthesis of silver nanoparticles and the study on catalytic activity in the degradation of dyes. *J. Mol. Liq.* **2015**, *204*, 184−191.
(42) Nguyen-Phan, T.-D.; Shin, E. W. Morphological effect of TiO_2 catalysts on photocatalytic degradation of methylene blue. *J. Ind. Eng. Chem.* **2011**, *17*, 397−400.
(43) Ramli, Z. A. C.; Asim, N.; Isahak, W. N.; Emdadi, Z.; Ahmad-Ludin, N.; Yarmo, M. A.; Sopian, K. Photocatalytic degradation of methylene blue under UV light irradiation on prepared carbonaceous TiO2. *Sci. World J.* **2014**, *2014*, 415136.
(44) Yang, H.; Zhang, K.; Shi, R.; Li, X.; Dong, X.; Yu, Y. Sol−gel synthesis of TiO_2 nanoparticles and photocatalytic degradation of methyl orange in aqueous TiO2 suspensions. *J. Alloys Compd.* **2006**, *413*, 302−306.
(45) Saravanan, R.; Manoj, D.; Qin, J.; Naushad, M.; Gracia, F.; Lee, A. F.; Khan, M. M.; Gracia-Pinilla, M. A. Mechanothermal synthesis of Ag/TiO_2 for photocatalytic methyl orange degradation and hydrogen production. *Process Saf. Environ. Prot.* **2018**, *120*, 339−347.
(46) Zheng, X.; Zhang, D.; Gao, Y.; Wu, Y.; Liu, Q.; Zhu, X. Synthesis and characterization of cubic Ag/TiO_2 nanocomposites for the photocatalytic degradation of methyl orange in aqueous solutions. *Inorg. Chem. Commun.* **2019**, *110*, 107589.
(47) Nasrollahzadeh, M. S.; Hadavifar, M.; Ghasemi, S. S.; Chamjangali, M. A. Synthesis of ZnO nanostructure using activated carbon for photocatalytic degradation of methyl orange from aqueous solutions. *Appl. Water Sci.* **2018**, *8*, 104.

https://doi.org/10.1021/acsomega.1c05090
ACS Omega 2022, 7, 4812−4820